

Scaling Laws in Self-Gravitating Disks

Daniel Huber & Daniel Pfenniger

Geneva Observatory, Ch. des Maillettes 51, CH-1290 Sauverny, Switzerland

Received / Accepted

Abstract.

The interstellar medium (ISM) reveals strongly inhomogeneous structures at every scale. These structures do not seem completely random since they obey certain power laws. Larson's law (1981) $\sigma \propto R^5$ and the plausible assumption of virial equilibrium justify to consider fractals as a possible description of the ISM. In the following we investigate how self-gravitation, differential rotation and dissipation affect the matter distribution in galaxies. To this end we have performed 3D-simulations for self-gravitating local boxes embedded in a larger disk, extending the 2D-method of Toomre & Kalnajs (1991) and Wisdom & Tremaine (1988). Our simulations lead to the conclusion that gravitation, shearing and dissipation can be dominantly responsible for maintaining an inhomogeneous and eventually a fractal distribution of the matter.

Keywords: Methods: numerical - Galaxies: ISM - ISM: structure

1. Introduction

The lumpy distribution of matter resulting in Toomre & Kalnajs' (1991, hereafter TK) local shearing-sheet experiments, reminds us of the ubiquitous inhomogeneous state of the ISM as well as the flocculent structures of many spirals. Therefore we decided to take up their 2D-model and to extend it on 3 dimensions order to investigate more precisely the clumpy structure of galactic matter. It is important to include the third dimension in the model, because as soon as clumping develops dynamical coupling with vertical motion must be strong, contrary to the weak coupling existing in a smoothly distributed thin disk. Our model considers scales of the order of $\mathcal{O}(1\text{kpc})$. Thus we are able to investigate the transition regime between the molecular cloud scales and the galactic disk scale. Furthermore we can investigate whether gravitation and dissipation can maintain the power laws observed in molecular clouds on scales at which shearing is dominant.

This paper is divided up in two main parts. The first part presents the model (Sects. 2.1-2.4) and the second part shows the results (Sect. 3.1) and their analysis, i.e. the determination of the fractal dimension (Sect. 3.2) and the verification of Larson's law (Sect. 3.3).



2. Model

2.1. PRINCIPLE

In local models only a small part (e.g., everything inside a box with a given size) of the system is simulated and more distant regions are represented by replicas of the local box. In such a model the orbital motion of the particles is determined by Hill's approximation of Newton's equations of motion (Hill 1878)

$$\begin{aligned} \ddot{x} - 2\Omega_0\dot{y} &= 4\Omega_0A_0x + F_x \\ \ddot{y} + 2\Omega_0\dot{x} &= F_y \\ \ddot{z} &= -\nu^2z + F_z \end{aligned} \quad (1)$$

where $A_0 = -\frac{1}{2}r_0\left(\frac{d\Omega}{dr}\right)_{r_0}$ is the Oort constant of differential rotation and ν is the vertical epicycle frequency. F_x, F_y and F_z are local forces due to the self-gravitating particles.

Because of the shearing flow the relative positions of the rectangular boxes (local box and replicas) change with time, so that a initially periodic arrangement of the boxes relative to a fixed Cartesian coordinate system can not be maintained. As a consequence the forces of the self-gravitating particles must be determined by direct summation, requiring $\mathcal{O}(N^2)$ operations for N particles.

To increase the performance in our models we calculate the forces with the FFT-convolution method, requiring $\mathcal{O}(N_c \log N_c)$ operations, where N_c is the number of cells, which should have the same order of magnitude as the number of particles. This requires a system spatially periodic at each time. Therefore we use a pair of time-dependent affine coordinate systems, whose affinity angle change with time and are determined by the shear flow (see Fig. 1). The angle difference between the two grids is constant and given by $\text{atan}(L_y/L_x)$. The reason to evaluate twice the forces in two different affine grids is for avoiding force discontinuities in time when the affine angle would have reached a maximum value beyond which a smaller angle would exist. After the calculation of the forces for the two affined grids, they are transformed into Cartesian coordinates, where they are weighted and added. The weighting factors are proportional to the grid inclination and normalized.

2.2. COOLING

To avoid an increase of the random epicyclic motion due to gravitational heating, TK proposed to add artificial cooling forces. Following them we include the damping terms $-C_x\dot{x}$ and $-C_z\dot{z}$ in the radial resp.

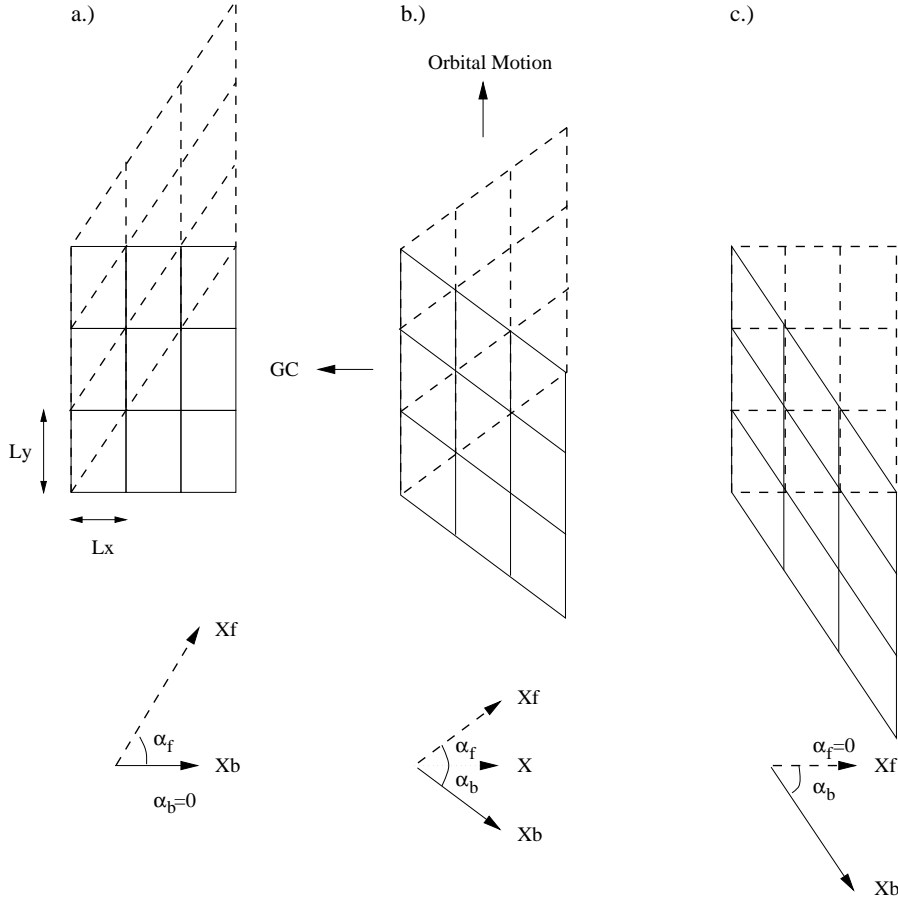


Figure 1. Schematic diagram of the inclined grids seen from above. *a.)* The initial state of the two grids ($t = 0$). The dashed grid is the forward grid and the solid one is the backward grid. Below them, the affinity angles of the grids are indicated, α_f resp. α_b . The angle between the two grids remains the same for all times. *b.)* The grids at $t = L_y/(2L_x\Omega_0)$, where $\alpha_f = -\alpha_b$. *c.)* When the grids attain these inclinations, they jump back to the positions shown in *(a)* and the process starts again without discontinuity in the dynamics.

vertical forces (F_x, F_z) controlling the particle motions via Eq. (1). Two different damping terms are necessary to reflect the different directional collision rates induced by the anisotropic velocity ellipsoid. The cooling coefficients are chosen in such a way that the velocity dispersions of the random motions reach a stable level and don't differ much from their initial values. The same stability conditions holds for the disk scale height z_0 .

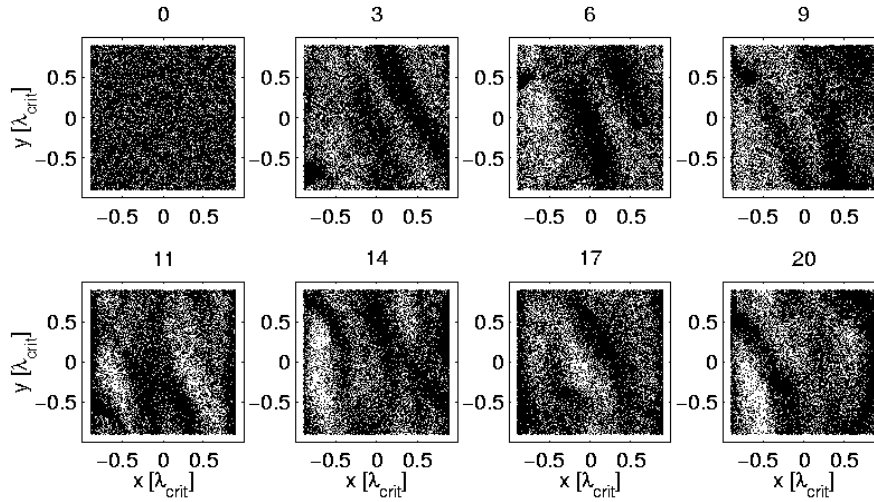


Figure 2. The evolution of the particle positions seen from above. The number of rotations of the shearing box around the galactic center are indicated above each panel. The number density at the beginning of the simulation is $n = 10100\lambda_{\text{crit}}^{-2}$, corresponding to 32724 particles.

3. Results

3.1. SHEARING BOXES

Fig. 2* and 3 reveals the spatial distribution of matter in a box, representing a section of a galactic disk. The size of the box sides ($L_x \times L_y \times L_z$) is given by the critical wavelength λ_{crit} , defining the scale for which the theory of swing amplification predicts the strongest response (Toomre 1981).

Because we are interested in long time behavior, the simulations were performed for $t = 20$ galactic rotations. In the initial state $t = 0$ the particles are distributed uniformly in the x-y-plane. The particle distribution in z -direction obeys $\rho \propto \text{sech}^2(z/z_0)$, where ρ is the density and z_0 is the disk scale height. The velocities at $t = 0$ are determined by the shear-flow

$$\dot{x} = 0, \quad \dot{y} = -2A_0x, \quad \dot{z} = 0 \quad (2)$$

and the Schwarzschild velocity ellipsoid.

* Full resolution paper available at <http://obswww.unige.ch/Preprints/cgi-bin/Preprintshtml.cgi?#DYNAMIC>.

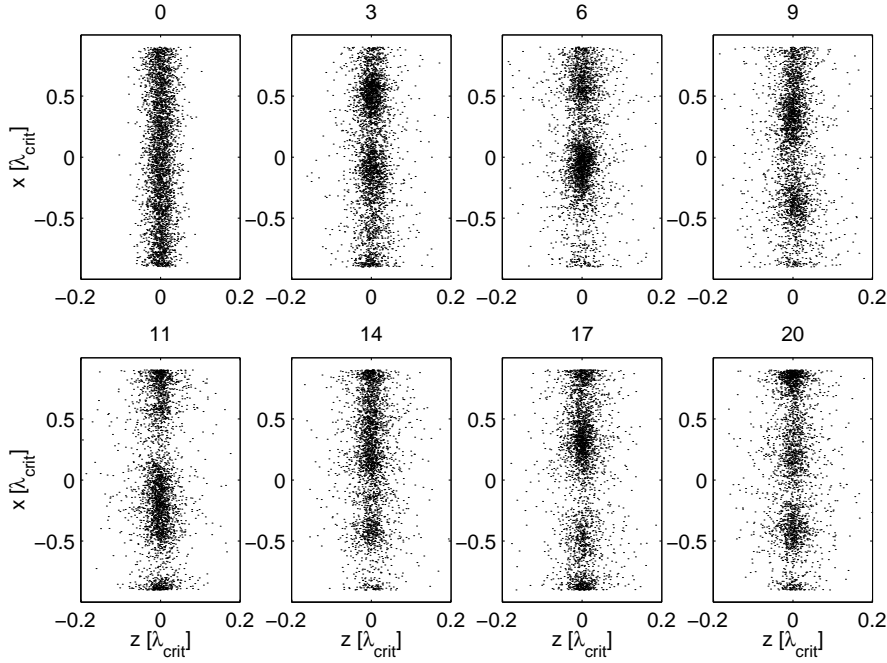


Figure 3. The positions of the particles inside the slice, $-0.1 \lambda_{\text{crit}} < y < 0.1 \lambda_{\text{crit}}$, seen in the direction of orbital motion.

Like the 2D-model of TK, our 3D-model reveals a fast “structure formation”. After the first rotations the striations are already developed and are more or less maintained during the rest of the simulation.

In our model $t_{\text{osc}} < t_{\text{cool},x} < t_{\text{cool},z}$ is valid, where t_{osc} is the period of the unforced epicyclic motion. $t_{\text{cool},x}$ and $t_{\text{cool},z}$ are the cooling times for the radial resp. vertical damping in fact $t_{\text{cool},x} \propto C_x^{-1}$ and $t_{\text{cool},z} \propto C_y^{-1}$. Furthermore, the cooling times depend on the particle number density n . For the simulation in Fig. 2 the following relation is valid: $t_{\text{osc}} : t_{\text{cool},x} : t_{\text{cool},z} \approx 1 : 40 : 300$.

The random velocity dispersions and the disk scale height were calculated after every half rotation and are plotted in Fig. 4. Gravitational instability and shearing, which are responsible for an important part of the striations, have an effect particularly in the x-y-plane and leads to a fast increase of σ_x and σ_y .

3.2. FRACTAL DIMENSION

During this studies our interest was particularly focused on the following question: Can self-gravitation, shearing and dissipation be dominantly responsible for maintaining a fractal distribution of the matter in a disk and can they account for Larson’s law (Larson 1981)? To

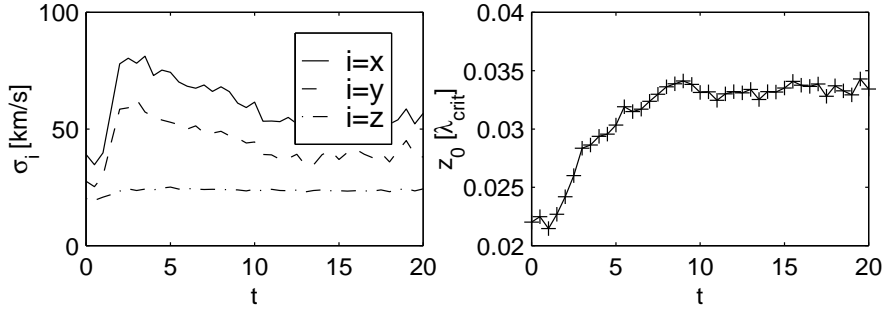


Figure 4. The left panel shows the velocity dispersions σ_x , σ_y and σ_z as a function of time t , indicated in galactic rotation unit. The right panel reveals the evolution of the disk scale height z_0 .

answer this question we calculated the appropriate scaling laws and determined the fractal dimension for the structures shown in Fig. 2 and 3.

We determined the fractal dimension, quantifying how much space our system fills, as follows: We choose a representative set of particles and count for each particle the number of neighboring particles $N(R)$ inside a certain radius R . If we repeat this for other values of R we can find the fractal dimension D via

$$N(R) \propto R^D. \quad (3)$$

Because the structures we examine are not an idealized mathematical set, but model a physical system, we have to take into account upper and lower cutoffs in the analysis. An upper limit due to the numerical model is given by the size of the simulation box in the x-y-plane. On this scale the system becomes periodic, meaning that it can not be fractal on scales $\mathcal{O}(L_x)$. A lower limit is due to the finite resolution of the box grid. If the grid cells have the size $l_x \times l_y \times l_z$ and $l = l_x = l_y > l_z$ then we can't expect fractal structures below $2l$. Fig. 5 reveals the fractal dimension $D = d\ln(N)/d\ln(R)$ as a function of the radius R , i.e. of the scale. The solid line corresponds to the initial distribution of matter: $\rho(x, y) = \text{const.}$, $\rho(z) \propto \text{sech}^2(z/z_0)$. The other lines give the mean dimensions of the structures for the simulation terminal phase. The intensity of the structures and thus the structure dimension D depend on the cooling. To show this clearly we performed simulations with varying cooling forces. The figure reveals clearly that the stronger the cooling, the more intensive the structures and the lower the structure dimension D are. The structures in Fig. 2 and 3 were performed with a “strong” cooling. For this structures D runs in a thin band between $0.2\lambda_{\text{crit}}$ and the upper model limit with a minimum of $D \approx 1.83$ at

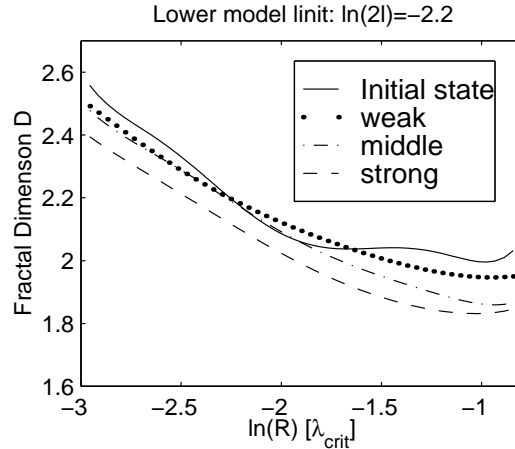


Figure 5. The structure dimension D as a function of the scale R . The solid line corresponds to the initial state. On large scales this state represents a 2D matter distribution, whereas on small scales $R < z_0$ it tends to $D > 2.6$. The other curves represent the simulation terminal phase for different cooling forces (weak, middle, strong). The relative magnitudes of the cooling coefficients are: $C_{x,\text{weak}} : C_{x,\text{middle}} : C_{x,\text{strong}} \approx 1 : 1.5 : 2$. Above the figure the natural logarithm of the lower model limit is indicated.

$R = 0.35\lambda_{\text{crit}}$. Pfenniger (1996) showed, that a fractal-like, hierarchical gravitating system in statistical equilibrium can only exist with $D < 2$. In the range, in which D runs in a thin band this condition is fulfilled, but the dynamical range is too small to call the structures fractals.

3.3. LARSON'S LAW

If the fractal organization of the matter extends to scales at which the shear flow becomes important and the system is still virialized, then the validity range of Larson's law

$$\sigma \propto R^\delta \quad \text{or} \quad \delta = \frac{d \ln \sigma}{d \ln R} \quad (4)$$

should exceed the size of Giant Molecular Clouds. We checked Larson's law for scales > 100 pc by analyzing the phase-space of the particles in Fig. 2.

Fig. 6 shows δ as a function of the scale R . There is no plateau between $0.3 < \delta < 0.5$, but δ reaches this range for the bigger scales, where also $2\delta + 1 = D$ is roughly fulfilled.

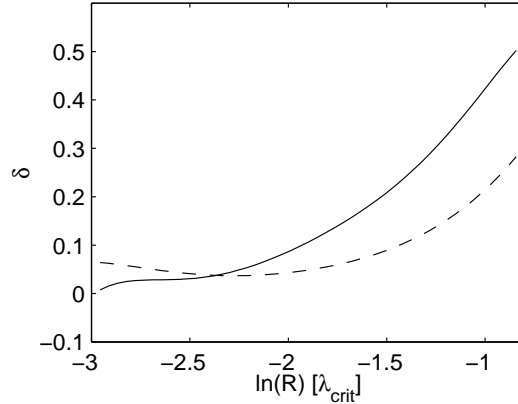


Figure 6. δ of Larson's law as a function of the scale R . To calculate δ we used the simulation with the particle density $n = 40450$ and the resolution $l = 0.03\lambda_{\text{crit}}$. The solid line corresponds to the initial state, whereas the dashed line indicates δ for the simulation terminal phase.

4. Conclusion

Our local 3D-simulations show, that self-gravitation and dissipation ensure a statistical equilibrium at scales at which the shear flow is important. Moreover they reveal a fractal-like distribution of matter on kpc-scales. The fractal dimension found in the simulations can be lower than 2, as observed in molecular clouds. The specific value found depends on the relative strengths of the competing gravitational and dissipation processes. Because the dynamical range of our simulations is still small, it would be premature to call the found structures strict fractals. The anisotropy of the velocity-dispersion ellipsoid, resulting from our simulations, has systematically the same ordering ($\sigma_R > \sigma_\Phi > \sigma_z$) as observed in the Galaxy and in N-body simulations of spirals.

Acknowledgements

This work has been supported by the Swiss Science Foundation.

References

- Larson R.B., 1981, MNRAS 194, 809
 Pfenniger D., 1996, in *New Extragalactic Perspectives in the New South Africa*, eds. D.L. Block and J.M. Greenberg, Kluwer Academic Publishers, Netherlands, p. 439

- Scalo J.M., 1985, in Protostars and Planets II, eds. Black D.C. and Matthews, Univ. of Arizona Press, p.201
- Toomre A., 1981, in The Structure and Evolution of Normal Galaxies, eds. Fall S.M. and Lynden-Bell D., Cambridge Univ. Press, p. 111
- Toomre A., Kalnajs A.J., 1991, in Dynamics of Disc Galaxies, ed. Sundelius B., Göteborg Univ. Press, p. 341
- Wisdom J., Tremaine S., 1988, Astron. J. 95, 925

